

SUPPORTING INFORMATION

Infrared multiple photon dissociation spectroscopy of a gas-phase oxo-molybdenum complex with 1,2-dithiolene ligands

Michael J. van Stipdonk^{1*}, Partha Basu^{1*}, Sara Dille¹, John K. Gibson², Giel Berden³ and Jos Oomens^{3,4}

¹Department of Chemistry and Biochemistry, Duquesne University, 600 Forbes Ave, Pittsburgh PA 15282 USA

²Chemical Sciences Division, Lawrence Berkeley National Laboratory, 1 Cyclotron Road, Berkeley, CA 94720 USA

³Radboud University Nijmegen, Institute for Molecules and Materials, FELIX Facility, Toernooiveld 7, 6525ED Nijmegen, The Netherlands

⁴van 't Hoff Institute for Molecular Sciences, University of Amsterdam, Science Park 904, 1098XH Amsterdam, The Netherlands

Figure S1. CID spectra generated from solution of $\text{MoO}(\text{mnt})_2^{2-}$: (a) CID (MS/MS stage) of m/z 524. (b) CID (MS^3 stage) of m/z 423 product derived from m/z 524 precursor.

Figure S2. CID spectra generated from solution of $\text{MoO}(\text{mnt})_2^{2-}$: (a) CID (MS/MS stage) of m/z 197, (b) CID (MS^3 stage) of m/z 394 product derived from m/z 197 precursor.

Figure S3. Comparison of IRMPD and predicted spectra for cyano-coordinated $\text{Mo}=\text{O}$: (a) structure III and (b) structure IV.

Figure S4. Data for IRMPD of $[\text{MoO}(\text{mnt})_2]^{2-}$: (a) experimental IRMPD spectrum and (b) predicted spectrum for $[\text{MoO}(\text{mnt})_2]^{2-}$ in singlet spin state at M06-L/6-311+G(d) level of theory. IRMPD spectrum is included as grey trace in (b) to facilitate comparison.

Figure S5. Data for IRMPD of $[\text{MoO}(\text{mnt})_2]^{2-}$: (a) experimental IRMPD spectrum and (b) predicted spectrum for $[\text{MoO}(\text{mnt})_2]^{2-}$ in singlet spin state at B3LYP/6-311+G(3df) level of theory. IRMPD spectrum is included as grey trace in (b) to facilitate comparison.

Figure S6. Data for IRMPD of $[\text{MoO}(\text{mnt})_2]^-$: (a) experimental IRMPD spectrum, (b) predicted spectrum for $[\text{MoO}(\text{mnt})_2]^-$ in doublet spin state and (c) predicted spectrum for $[\text{MoO}(\text{mnt})_2]^-$ in quartet spin state. Predicted spectra are from calculations at the M06-L/6-311+G(d) level of theory. IRMPD spectrum is included as grey trace in (b) and (c) to facilitate comparison.

Figure S7. Data for IRMPD of $[\text{MoO}(\text{mnt})_2]^-$: (a) experimental IRMPD spectrum, (b) predicted spectrum for $[\text{MoO}(\text{mnt})_2]^-$ in doublet spin state and (c) predicted spectrum for $[\text{MoO}(\text{mnt})_2]^-$ in quartet spin state. Predicted spectra are from calculations at the B3LYP/6-311+G(3df) level of theory. IRMPD spectrum is included as grey trace in (b) and (c) to facilitate comparison.

Figure S8. General structure for $\text{MoO}(\text{mnt})_2^{n-}$ with atom labels

Table S1. Dihedral angles predicted for $\text{MoO}(\text{mnt})_2^-$ and $\text{MoO}(\text{mnt})_2^{2-}$.

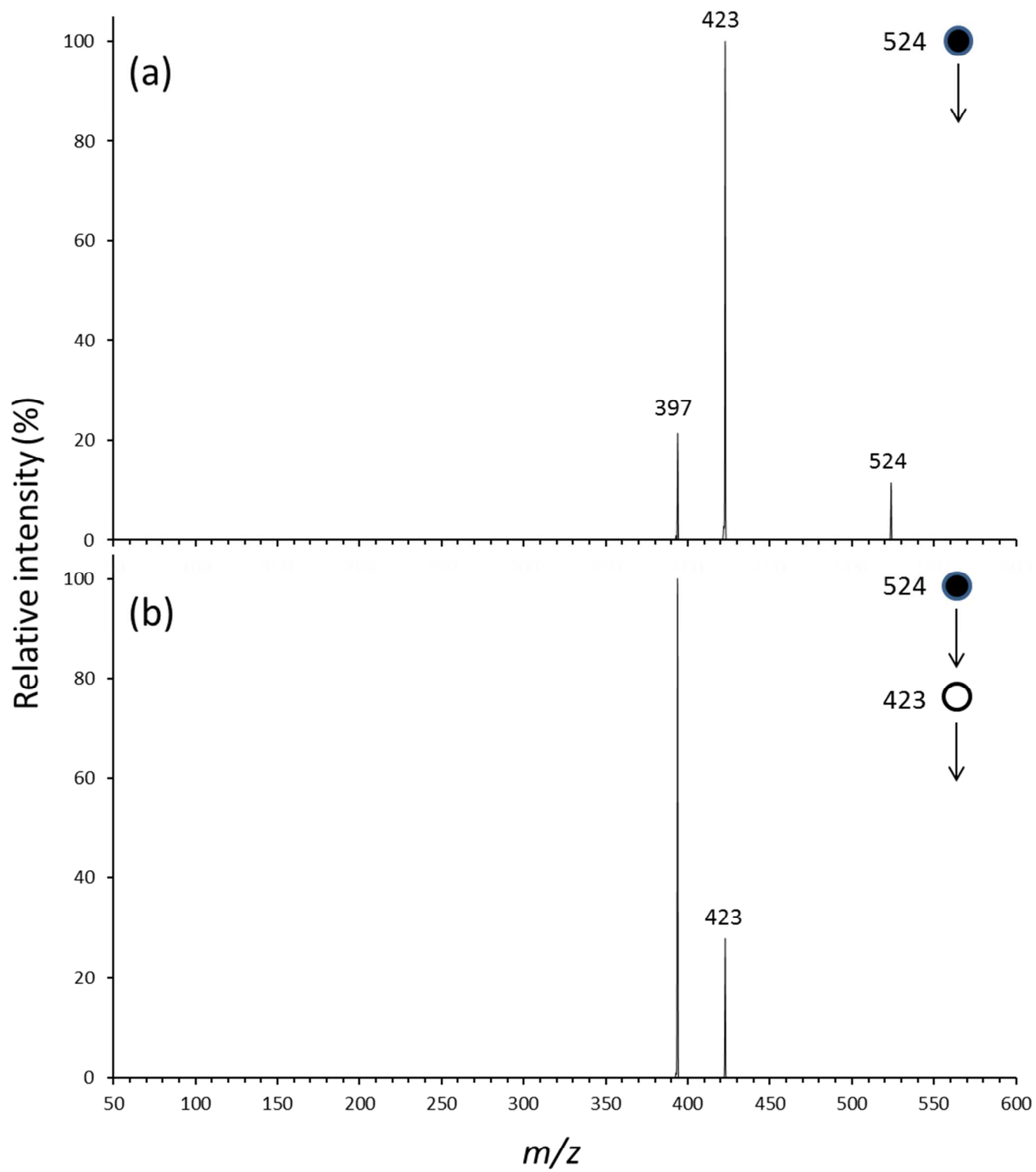


Figure S1.

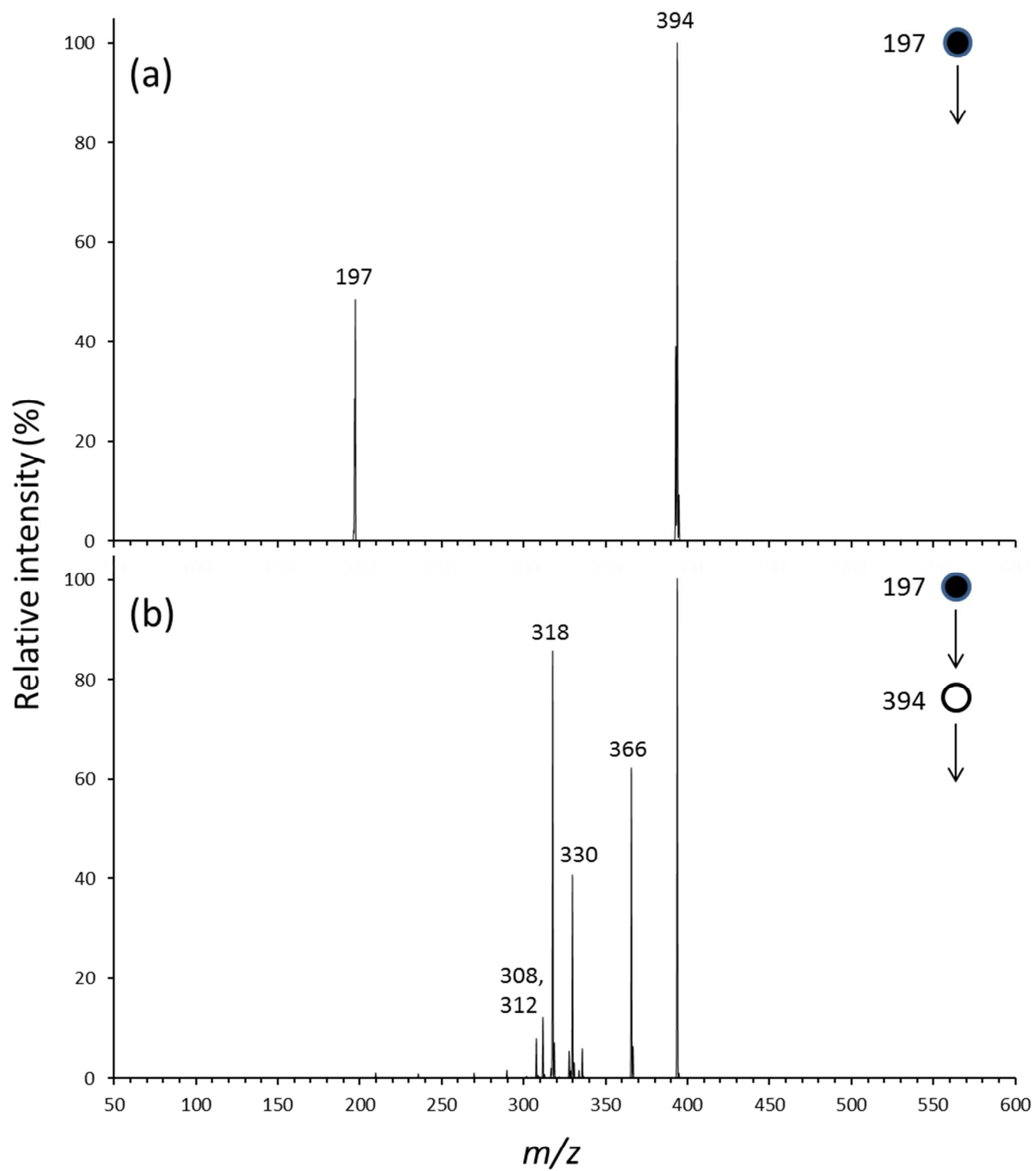


Figure S2.

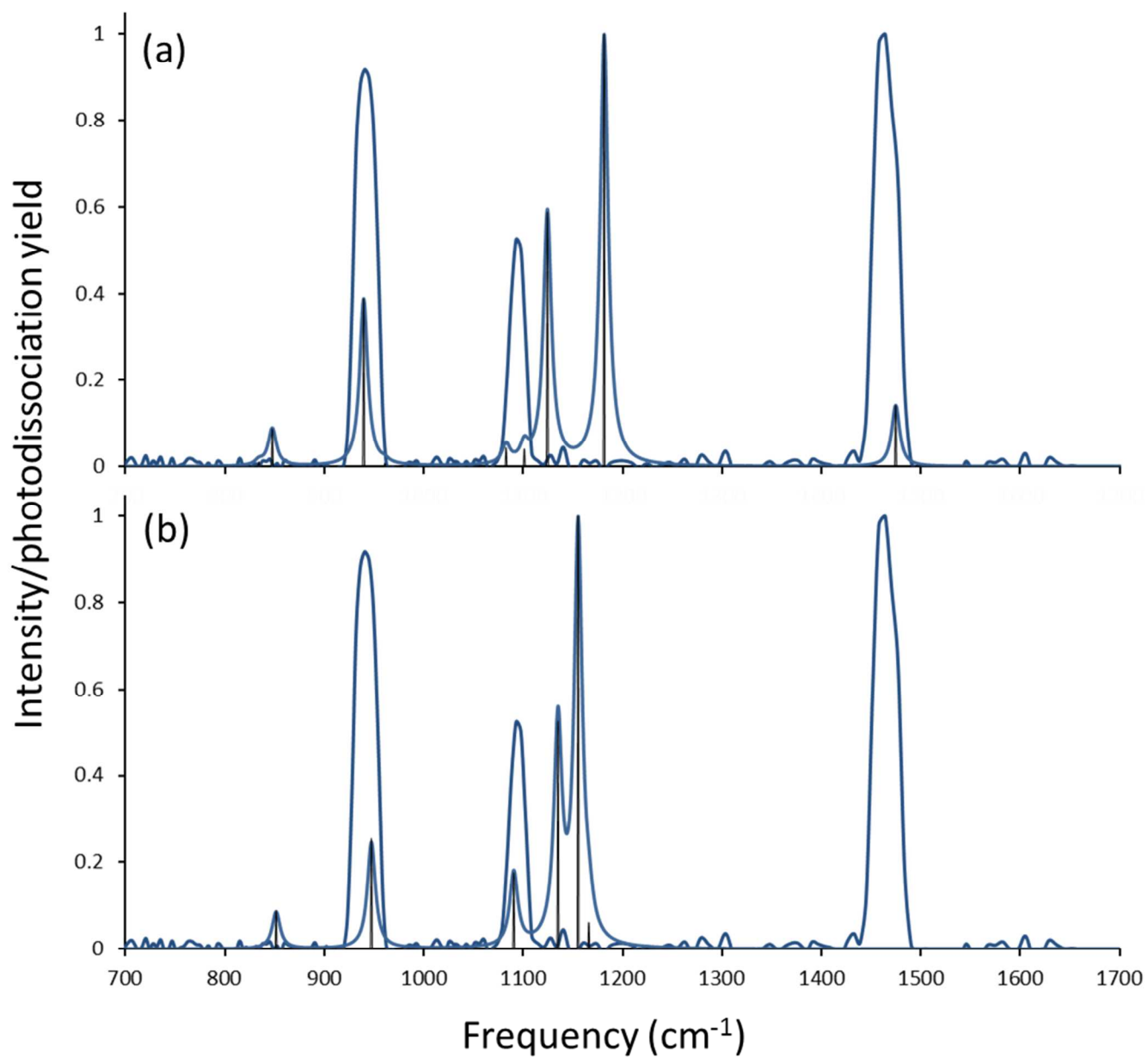


Figure S3.

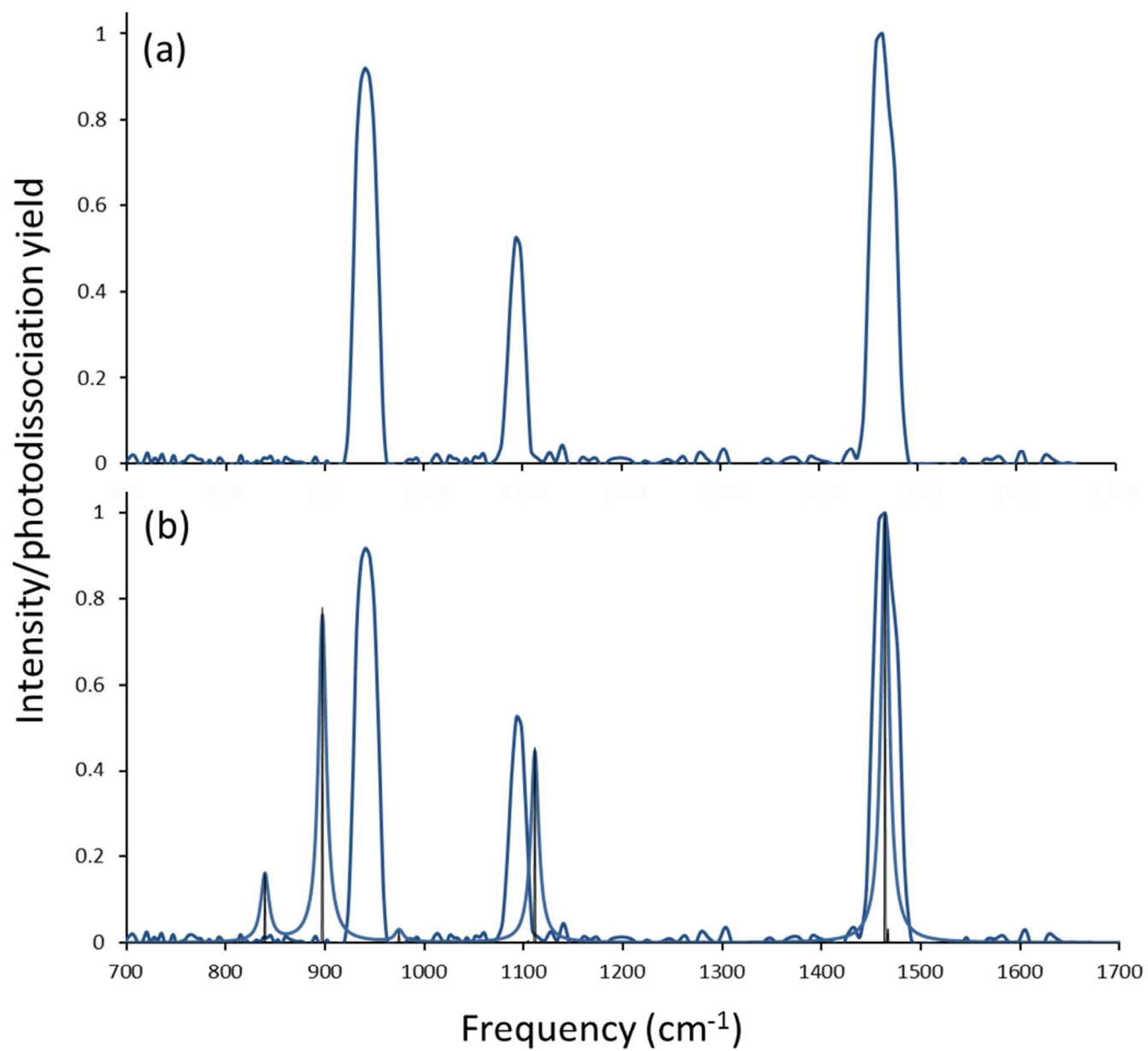


Figure S4.

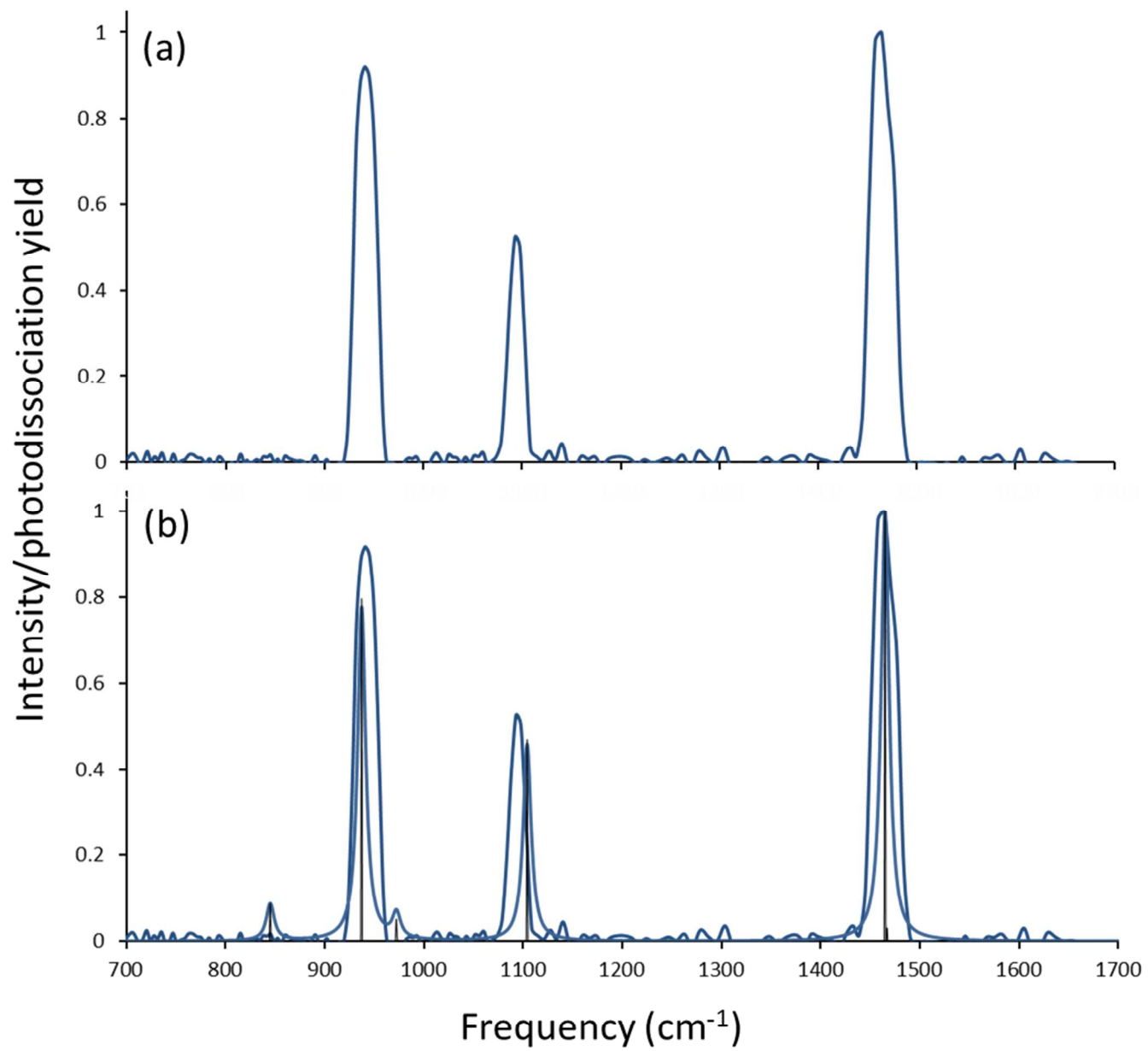


Figure S5.

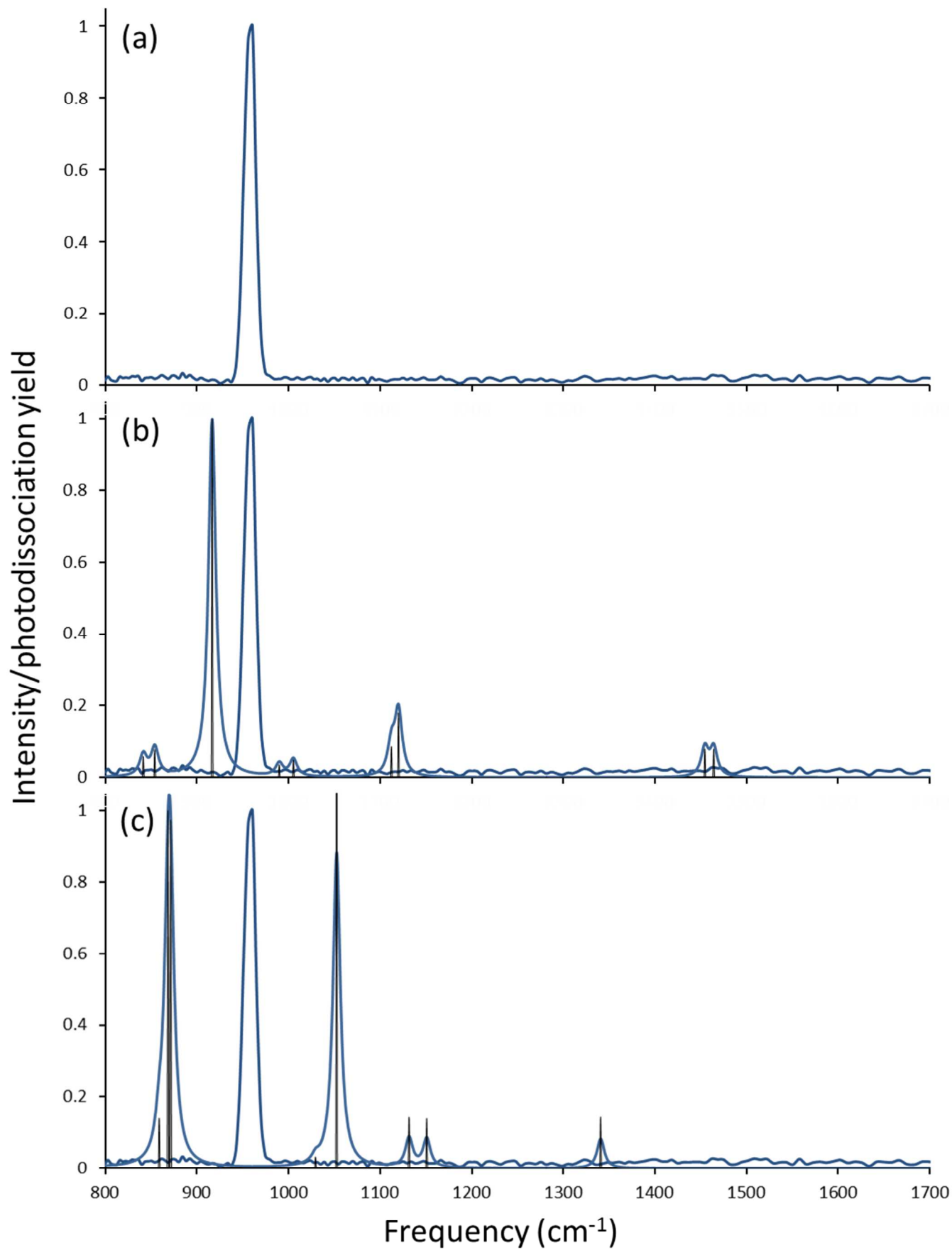


Figure S6.

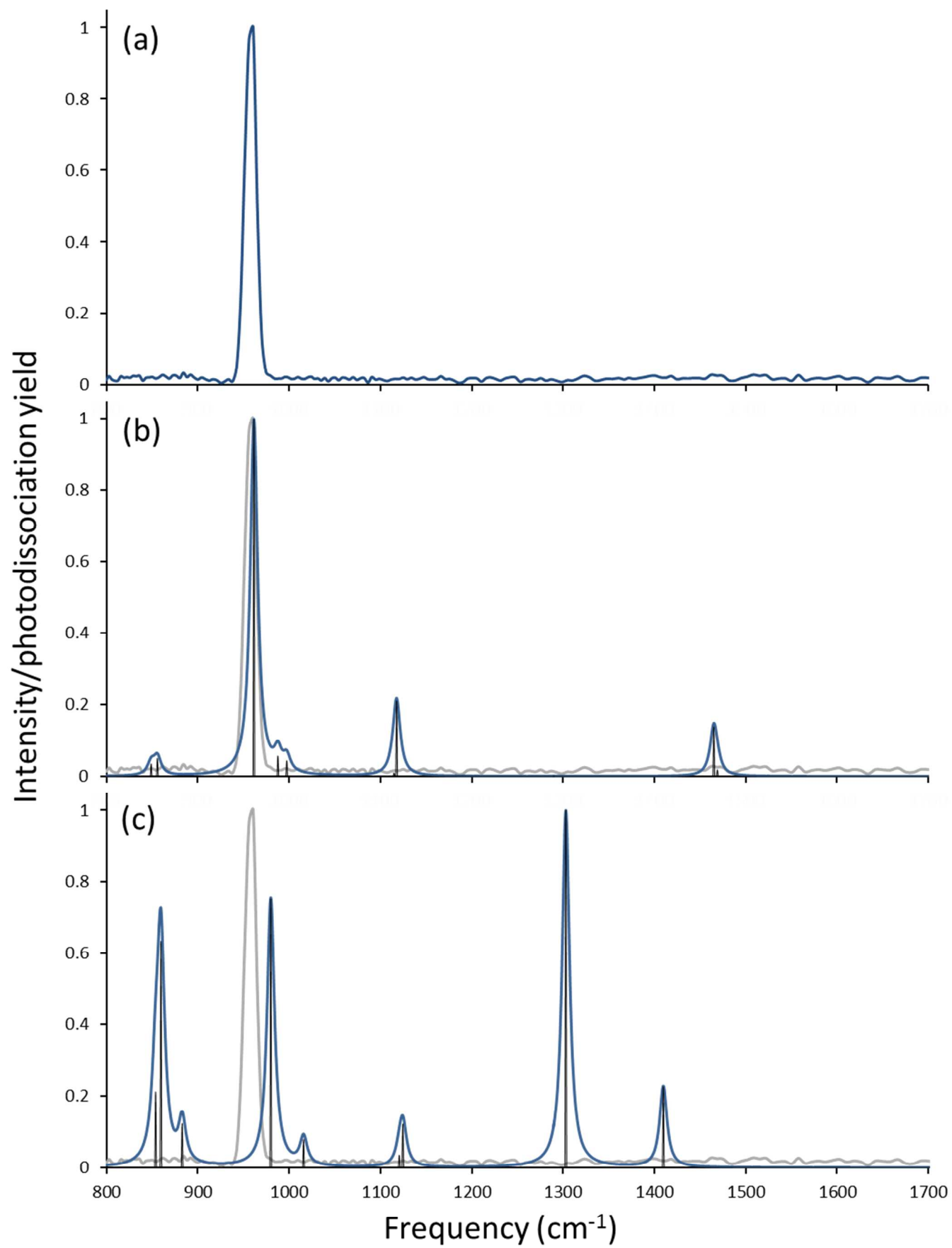


Figure S7.

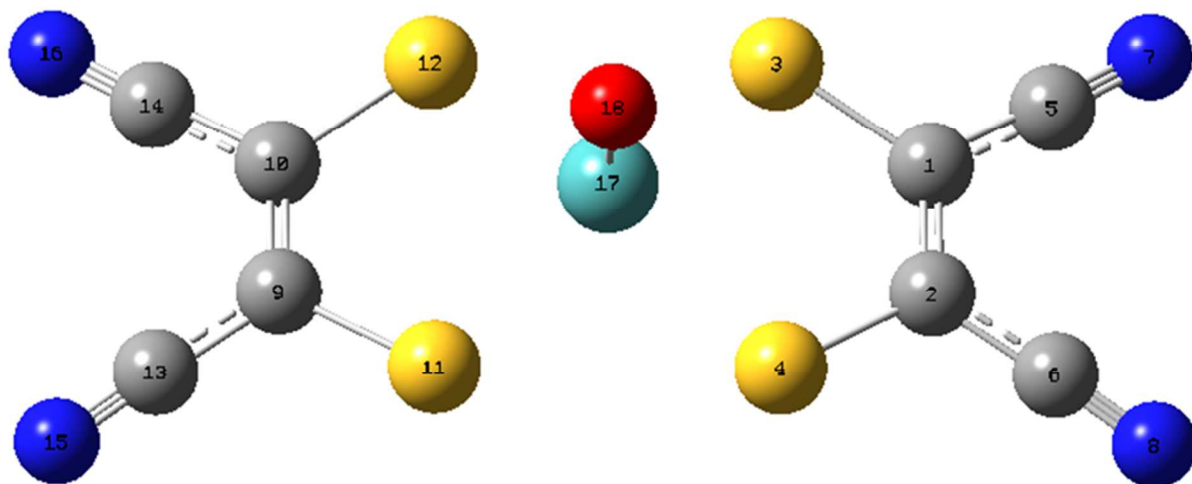


Figure S8.

Table S1.

[MoO(mnt) ₂] ²⁻ , singlet	D18-17-12-10	D18-17-11-9	D18-17-3-1	D18-17-4-2
B3LYP/6-31G(d)	-95.07	95.07	95.07	-95.07
B3LYP/6-311+G(d)	-95.42	95.42	95.41	-95.42
B3LYP/6-311+G(3df)	-95.55	95.55	95.53	-95.53
M06-L/6-311+G(d)	-95.67	95.68	95.68	-95.67
[MoO(mnt) ₂], doublet	D18-17-12-10	D18-17-11-9	D18-17-3-1	D18-17-4-2
B3LYP/6-31G(d)	-114.51	114.51	80.56	-80.56
B3LYP/6-311+G(d)	-115.00	115.00	81.23	-81.23
B3LYP/6-311+G(3df)	-114.38	114.37	81.75	-81.75
M06-L/6-311+G(d)	-114.85	114.85	79.25	-79.25
[MoO(mnt) ₂], quartet	D18-17-12-10	D18-17-11-9	D18-17-3-1	D18-17-4-2
B3LYP/6-31G(d)	-108.45	117.21	124.06	-75.58
B3LYP/6-311+G(d)	-108.61	117.94	125.03	-76.03
B3LYP/6-311+G(3df)	-109.02	116.51	123.92	-75.54
M06-L/6-311+G(d)	-108.82	120.19	133.65	-76.66